The contribution of distant sources to the observed flux of ultra high-energy cosmic rays

Ellis R. Owen[1,2], Qin Han[3,4], Kinwah Wu[4,5] , Y. X. Jane Yap[1], Pooja Surajbali[6]

[1]Institute of Astronomy, National Tsing Hua University, Hsinchu, Taiwan (ROC)
[2]Center for Informatics and Computation in Astronomy, National Tsing Hua University, Hsinchu, Taiwan (ROC)
[3]School of Astronomy and Space Science, Nanjing University, 163 Xianlin Avenue, Nanjing, Jiangsu 210093, PR China
[4]Mullard Space Science Laboratory, University College London, Holmbury St. Mary, Dorking, Surrey RH5 6NT, United Kingdom
[5]Research Center for Astronomy, Astrophysics and Astrophotonics, Macquarie University, Sydney, NSW 2109, Australia
[6]Max-Planck-Institut für Kernphysik, Saupfercheckweg 1, Heidelberg 69117, Germany

天文研究所 Institute of Astronomy

國立清華大學 NATIONAL TSING HUA UNIVERSITY

The Universe is opaque to UHE CRs of energies ~(10^{18}-10^{20}) eV over a few tens of Mpc, due to their interaction with background radiation fields. This sets the Greisen-Zatsepin-Kuz'min (GZK) horizon. Here, we show that a non-negligible fraction of the UHE CRs arriving on Earth could originate from beyond this horizon when heavy nuclear CRs, and the population and evolution of UHE CR sources are taken into account. This leads to the natural emergence of an isotropic UHE CR background.

1 Introduction

The detection rate of ultra high-energy (UHE) cosmic ray (CR) events on Earth is about 1 particle per square km per century at 10^{20} eV, corresponding to a flux of $E^3 J(E) \approx 10^{24}\mathrm{eV}^2\mathrm{m}^{-2}\mathrm{s}^{-1}\mathrm{sr}^{-1}$ (Ivanov et al. 2017). Several origins of these particles have been proposed, where conditions exist to allow acceleration of particles to ultra-high energies over large scales or in strong magnetic fields, such as in the relativistic jets of active galactic nuclei (AGN), neutron stars and in the large-scale shocks associated with galaxy clusters. However, their exact origins remain unsettled.

The low flux of UHE CRs is attributed both to the power-law nature of their intrinsic emission spectra from plausible sources, coupled with the attenuation of cosmologically propagating UHE particles with ambient radiation fields (cf. the *Greisen-Zatsepin-Kuz'min*, GZK, effect – Greisen 1966; Zatsepin & Kuz-min 1966). This is mainly caused by hadronic interactions with the cosmological microwave background (CMB) and, to a lesser extent, the infra-red and optical components of the extra-galactic background light (EBL). Through **photo-pair**, **photo-pion** and **photo-spallation** interactions, the Universe becomes 'optically thick' to UHE CRs over distances of a few 10s Mpc (see Figure 1), setting a GZK `horizon' beyond which substantial attenuation would be expected. The extent of this horizon depends on the energy and nuclear mass of a CR.

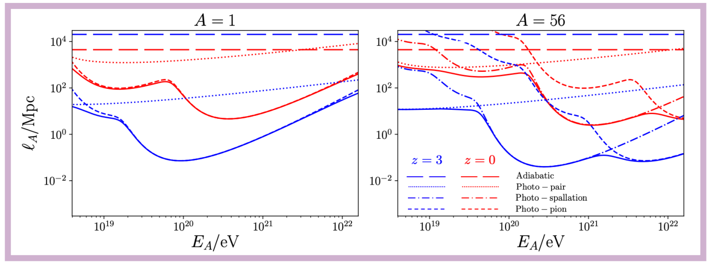

Figure 1: *The characteristic lengths of energy-loss for nuclei traversing through background (CMB and EBL) cosmological radiation fields for various cooling and absorption processes (as labelled). Red lines denote distances computed at z=0, while blue lines are distances computed at z=3. The left plot shows the case for ¹H, and right for ⁵⁶Fe.*

2 Source Populations

The UHE CR injection rate by source populations may be written as:

$$Q^{\mathrm{a}}_A(z,\epsilon_A,A) = C_0(1+z)^{-3}\psi_{\mathrm{x}}(z)\frac{\mathrm{d}}{\mathrm{d}\epsilon_A}\left(\frac{\mathrm{d}n^\star}{\mathrm{d}t}\right)$$

where Q^a_A is the (comoving) source term, $\psi_x(z)$ is the evolutionary function describing the distribution of a CR source population with respect to redshift z (the specific model is denoted by subscript x – see Figure 2 for the 4 source models we consider, following Alves Batista et al. 2019). The normalization C_0 is set by the UHE CR luminosity density:

$$\rho_{\mathrm{CR}} = C_0 \sum_A \int_{\epsilon_{\mathrm{min}}}^{\epsilon_{\mathrm{max}}} \mathrm{d}\epsilon_A\, \epsilon_A \psi_{\mathrm{x}}(z)\frac{\mathrm{d}}{\mathrm{d}\epsilon_A}\left(\frac{\mathrm{d}n^\star}{\mathrm{d}t}\right)\bigg|_{z=0}$$

which we treat as a model parameter, with values given by Table 1 for each considered source model. The volumetric spectral injection rate of CRs by a given source population, with a parametrised injection spectrum is given by:

$$\frac{\mathrm{d}n^\star}{\mathrm{d}\epsilon_A} \propto f_A\left(\frac{\epsilon_A}{\epsilon_{\mathrm{min}}}\right)^{-\alpha}\begin{cases}1 & (x<1)\\ \exp(1-x) & (x\geq 1)\end{cases}$$

where $x = \epsilon_A m_e c^2/Z_A R_{\max}$, $R_{\max}$ is the rigidity, and the energy limits are $\epsilon_{\min} m_e c^2 = 3.98\times 10^{18}$ eV, and $\epsilon_{\max} m_e c^2 = 3.16\times10^{20}$ eV. The values of the spectral index α and the rigidity are shown in Table 1. The spectral composition adopts fitted values obtained by Alves Batista et al. 2019, where the full range of injected species are represented by abundances of ^{1}H, ^{4}He, ^{14}N, ^{28}Si and ^{56}Fe.

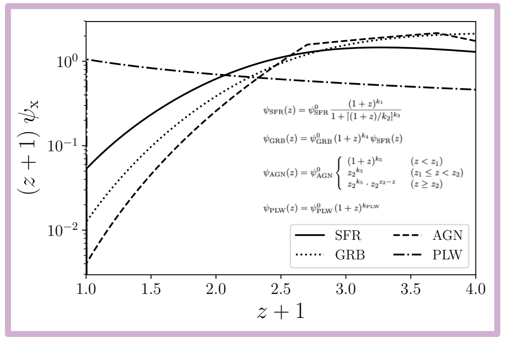

Figure 2: *Redshift distributions of the four source models, SFR, GRB, AGN and PLW. Their corresponding normalized redshift evolution functions are indicated where, for the SFR model $k_1 = 2.7$, $k_2 = 2.9$ and $k_3 = 5.6$, for the GRB model $k_4 = 1.4$, for the AGN model $k_5 = 5.0$, $z_1 = 1.7$, $z_2 = 2.7$, and for the PLW model $k_{\mathrm{PLW}} = -1.6$.*

Model	Normalisation ψ^0_{x}	Spectral index α	$\log(R_{\max}/V)$	$\rho_{\mathrm{CR}}/10^{48}$ erg Mpc^{-3} yr^{-1}
(1) SFR	$\psi^0_{\mathrm{SFR}} = 0.054$	−1.3	18.2	0.5
(2) GRB	$\psi^0_{\mathrm{GRB}} = 0.013$	−1.5	18.2	2.0
(3) AGN	$\psi^0_{\mathrm{AGN}} = 0.0041$	−1.0	18.2	0.04
(4) PLW	$\psi^0_{\mathrm{PLW}} = 1.1$	+1.0	18.7	15.0

Table 1: *Summary of parameter choices adopted for each of the four redshift source distribution models.*

3 UHE CR Propagation

The CR spectrum, expected to be observed at z=0, is computed by numerically solving the transport equation under a quasi-steady condition for each of the four source models:

$$\frac{\partial n_A}{\partial z} = \frac{1}{c}\left[\frac{\partial}{\partial \epsilon_A}(b_A n_A) + Q_A - \Lambda_A n_A\right]\frac{\mathrm{d}s}{\mathrm{d}z}$$

The numerical integration proceeds from $z_{\max} = 3$ to $z_{\min} = 0$. Here, $\mathrm{d}s/\mathrm{d}z$ is set by the adopted cosmological model (ΛCDM), primary CR injection as well as secondary nuclear production arising from interactions is encoded into the source term, where $Q_A = Q_A^{\mathrm{sp}}(z,\epsilon_A) + Q_A^{\mathrm{a}}(z,\epsilon_A)$ for $Q_A^{\mathrm{a}} = Q_A^{\mathrm{a}}(1+z)^3$ as the injection term of UHE CRs from the source population, and $Q_A^{\mathrm{sp}}(z,\epsilon_A)$ is the injection term of secondary UHE CRs arising from photo-degradation interactions (not applicable to ^{1}H).

Figure 3 shows the UHE CR spectrum z=0 in the case of the four source population models. Data obtained by the Pierre Auger Observatory (PAO 2019) are included for comparison, which demonstrates good consistency of our model with observations for all four source populations. The spectra at z=0 in each case are similar, with a shape almost identical to the injected spectra.

Figure 3: *Flux spectra of CRs for the source models, SFR, GRB, AGN and PLW propagated to z=0 for all nuclear species. The data (discrete red data points with error bars) obtained by the Pierre Auger Observatory (PAO 2019) are shown for comparison.*

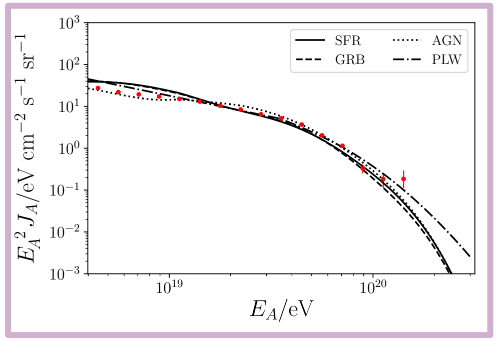

4 Results

Figure 4 shows the fractional contribution from sources above a given redshift, $f_{\mathrm{CR}}(>z)$, for the four source models. This demonstrates, in all cases, a large faction of UHE CR flux observed at Earth can not be attributed to local sources, regardless of the uncertainties in existing models of the EBL at high redshift or CR composition. Moreover, the curves for the GRB and AGN models are practically indistinguishable. This is because the curve is a manifestation of where the redshift locations of the underlying source population make the most significant contribution to the UHE CR flux. The dominant redshift locations of the GRB and AGN CR sources are very similar to one another (see Figure 2) which, together with the small numbers of GRBs and AGN below $(z+1)\sim2.5$ leads to their almost identical $f_{\mathrm{CR}}(>z)$ curves.

Figure 4: *The fraction of CRs that originate from redshift higher than z, $f_{\mathrm{CR}}(>z)$, for the four source models. The bottom abscissa shows the redshift z, and the top abscissa shows corresponding distances.*

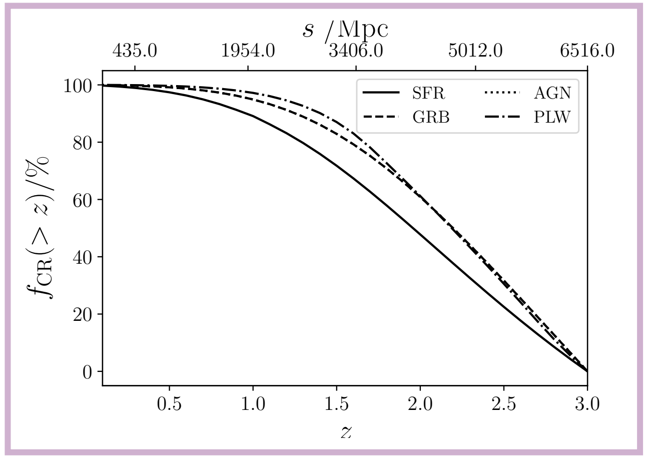

Our calculations show that **distant UHE CR sources at redshifts as high as z~(2-3) contribute substantially to UHE CRs detected on Earth**, naturally leading to the formation of a strong, diffuse isotropic background in the UHE CR flux. Only limited anisotropies would emerge, due to flux from nearby CR accelerators (within the GZK horizon) being superposed onto this background.

Moreover, we find that **most of the UHE CRs from these distant sources are primary particles, despite the large cosmological distances that they have traversed,** with their spectra and composition at $z = 0$ being almost indistinguishable from that injected by the source population, even when fully accounting for photo-spallation of nuclei along CR propagation paths.

We find our results to be robust, and **not strongly dependent on CR composition, source redshift distribution (if reasonable) or EBL intensity** up to redshifts as high as $z\sim3$.

References: *Alves Batista et al. 2019 JCAP (1) 002; Greisen 1966, PhRvL 16:748; Ivanov et al. 2017, PoS(ICRC2017)498; Pierre Auger Collaborataion (PAO) 2019, PAO contributions to the 36th International Cosmic Ray Conference (ICRC 2019), arXiv: 1909.09073; Zatsepin & Kuz'min 1966, Soviet Journal of Experimental and Theoretical Physics Letters, 4:78.*